

# Substrate Recognition and Selection by the Initiation Module PheATE of Gramicidin S Synthetase

Lusong Luo, Michael D. Burkart, Torsten Stachelhaus,<sup>†</sup> and Christopher T. Walsh\*

Contribution from the Department of Biological Chemistry and Molecular Pharmacology, Harvard Medical School, 240 Longwood Avenue, Boston, Massachusetts 02115

Received July 19, 2001

**Abstract:** The initiation module of non-ribosomal peptide synthetases (NRPS) selects and activates the first amino acid and serves as the aminoacyl donor in the first peptide bond-forming step of the NRPS assembly line. The gramicidin S synthetase initiation module (PheATE) is a three-domain subunit, recognizing L-phenylalanine (L-Phe) and activating it (by adenylation domain) as tightly bound L-phenylalanyl-adenosine-5'-monophosphate diester (L-Phe-AMP), transferring it to the HS-phosphopantetheine arm of the holo-thiolation (holo-T) domain, and then epimerizing it (by epimerization domain) to the D-Phe-S-4'-Ppant-acyl enzyme. In this study, we have assayed the selectivity of the PheATE adenylation domain with a number of proteinogenic amino acids and observed that three additional amino acids, L-Tyr, L-Trp, and L-Leu, were activated to the aminoacyl-AMPs and transferred to the HS-phosphopantetheine arm of the holo-T domain. Hydrolytic editing of noncognate aminoacyl-AMPs and/or aminoacyl-S-4'-Ppant-acyl enzymes by the enzyme was not observed by three different assays for adenylation domain function. The microscopic reaction rates and thermodynamic equilibrium constants obtained from single-turnover studies of reactions of L-Phe, L-Trp, L-Tyr, and L-Leu with holoPheATE allowed us to construct free energy profiles for the reactions, revealing the kinetic and thermodynamic basis for substrate recognition and selection. In particular, the rates of epimerization of the L-aminoacyl-S-enzyme to the D-aminoacyl-S-enzyme intermediate showed reductions of 245-, 300-, and 540-fold for L-Trp, L-Tyr, and L-Leu respectively, suggesting that the epimerization domain is an important gatekeeper for generation of the D-Phe-S-enzyme that starts gramicidin S chain growth.

## Introduction

Nonribosomal peptides, which constitute a large family of natural products that include numerous clinically invaluable drugs such as vancomycin (antibacterial), bleomycin (antitumor), and cyclosporin (immunosuppressant), are biosynthesized enzymatically by non-ribosomal peptide synthetases (NRPS) via thiotemplating on multimodular multidomain enzymatic assembly lines.<sup>1,2</sup> The number and organization of the iterated modules, which form both the NRPS template and the catalyst,

dictate the primary structure, size, and complexity of the non-ribosomal peptides.<sup>3</sup> Each module in this thiotemplate is composed of a linear arrangement of conserved core domains (see Figure 1, for example), which are involved in amino acid substrate recognition and adenylation (A domain), cofactor 4'-phosphopantetheine (Ppant)-dependent thiolation (T domain or peptidyl-carrier protein (PCP)), and condensation (C domain). In addition to those core domains, auxiliary domains that can modify the growing peptide chain (e.g., epimerization, cyclization, methylation, and N-acylation) are encased in some of the modules, which dramatically increase the diversity and versatility of non-ribosomal peptides.<sup>4</sup> Previous biochemical and structural studies have shown that major fidelity or editing functions for amino acid activation, selection, and incorporation into the elongating peptide chain reside in the A domains of NRPS.<sup>5,6</sup> Recently, selectivity of C domains toward donor and acceptor substrates has been investigated by small-molecule surrogates or construction of hybrid synthetases via domain/module fusions.<sup>7–9</sup> The observed stereoselective (L- vs D-) and size-based discrimination in addition to the differential selectiv-

\* To whom correspondence should be addressed. Phone: (617) 432 1715. Fax: (617) 432 0438. E-mail: christopher\_walsh@hms.harvard.edu.

<sup>†</sup> Present address: Institute of Biochemistry, Department of Chemistry, Philipps-University Marburg, Hans-Meerwein-Str., 35032 Marburg, Germany.

(1) Abbreviations used: GrsA, gramicidin S synthetase A; GrsB, gramicidin S synthetase B; L-Phe, L-phenylalanine; Ppant, 4'-phosphopantetheine; aa-S-Ppant-T, aminoacylated thioester form of cofactor Ppant-modified holo T domain; A, adenylation domain; T, thiolation domain; E, epimerization domain; ATE, adenylation–thiolation–epimerization domains; L-Phe-AMP, L-phenylalanyl-adenosine-5'-phosphate diester; AMP, adenosine 5'-monophosphate; ADP, adenosine 5'-diphosphate; ATP, adenosine 5'-triphosphate; Hepes, N-(2-hydroxyethyl)piperazine-N'-2-ethanesulfonic acid; NMR, nuclear magnetic resonance; Pi, inorganic phosphate; PPI, inorganic pyrophosphate; PPI-ase, inorganic pyrophosphatase; MesG, 2-amino-6-mercapto-7-methylpurine ribonucleoside; PNP, purine nucleoside phosphorylase; BSA, bovine serum albumin; C, condensation domain; CoA or CoASH, coenzyme A; HPLC, high-performance liquid chromatography; LSC, liquid scintillation counting; TCEP, tris(2-carboxyethyl)phosphine; TCA, trichloroacetic acid; TLC, thin-layer chromatography; NRPS, non-ribosomal peptide synthetase; PheA, adenylation domain construct of the PheATE module; a.a., amino acid; pant, pantetheine; a.a.-pant, aminoacyl-S-pantetheine.

(2) (a) Cane, D. E.; Walsh, C. T. *Chem. Biol.* **1999**, *6*, R319–325. (b) Marahiel, M. A.; Stachelhaus, T.; Mootz, H. D. *Chem. Rev.* **1997**, *97*, 2651–2673.

(3) Vondohren, H.; Keller, U.; Vater, J.; Zocher, R. *Chem. Rev.* **1997**, *97*, 2675–2705.

(4) Konz, D.; Marahiel, M. A. *Chem. Biol.* **1999**, *6*, R39–48.

(5) Stachelhaus, T.; Mootz, H. D.; Marahiel, M. A. *Chem. Biol.* **1999**, *6*, 493–505.

(6) Conti, E.; Stachelhaus, T.; Marahiel, M. A.; Brick, P. *EMBO J.* **1997**, *16*, 4174–4183.

(7) Belshaw, P. J.; Walsh, C. T.; Stachelhaus, T. *Science* **1999**, *284*, 486–489.

(8) Ehmman, D. E.; Trauger, J. W.; Stachelhaus, T.; Walsh, C. T. *Chem. Biol.* **2000**, *7*, 765–772.

(9) Linne, U.; Marahiel, M. A. *Biochemistry* **2000**, *39*, 10439–10447.

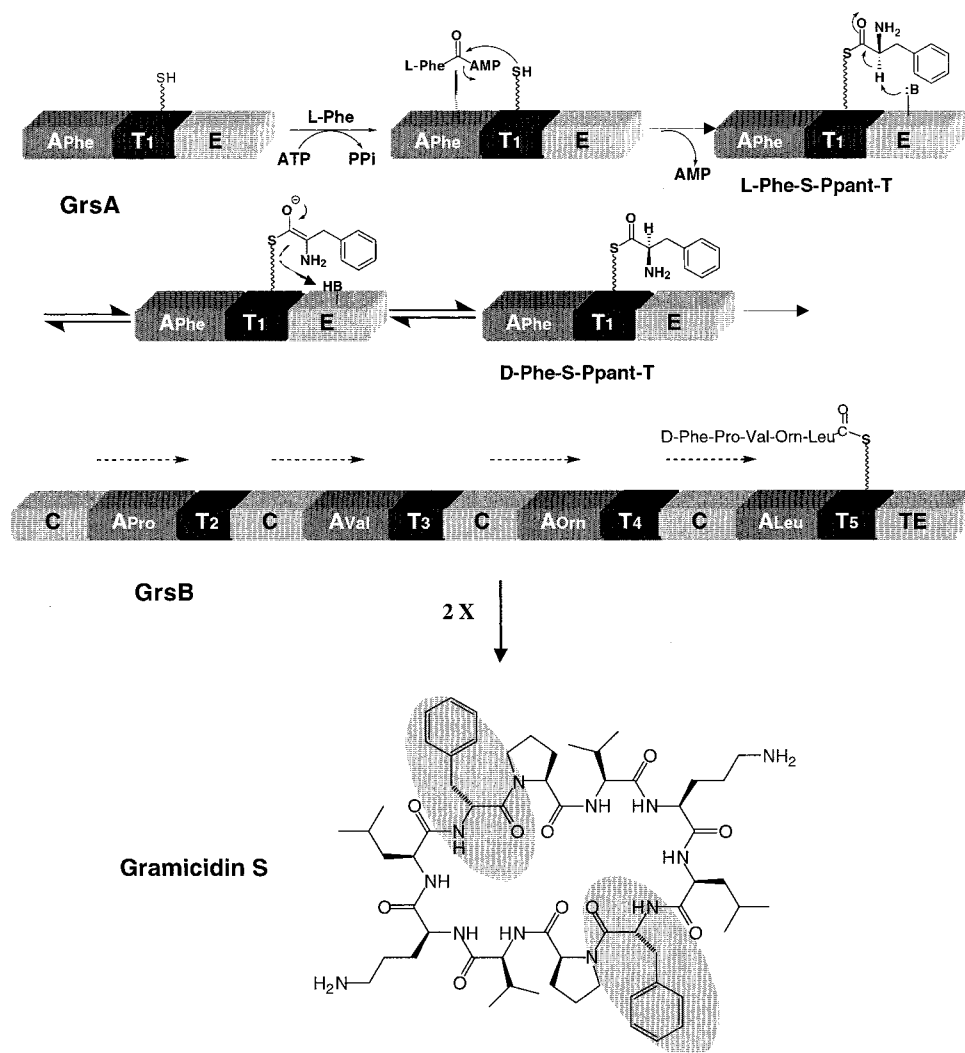


**Figure 1.** Biosynthesis of gramicidin S by GrsA and GrsB. In GrsA, a tightly bound intermediate L-Phe-AMP is first formed by the adenylation of L-Phe with ATP·Mg<sup>2+</sup> catalyzed by the A domain. The amino acyl group is then transferred to the Ppant arm of the T domain and subsequently epimerized at the active site of the E domain in the amino acyl-Ppant-acyl enzyme form, giving a 2:1 equilibrium mixture of D-/L-Phe-S-Ppant-enzyme adducts.<sup>12,13</sup> The D-Phe-S-Ppant-enzyme is accepted by the downstream C domain for transfer to the next module ProCAT in GrsB. After another three elongation steps, the pentapeptidyl-enzyme is formed and then dimerized and cyclized to release gramicidin S. The D-Phe incorporated by GrsA in the gramicidin S structure is highlighted.

ity at the donor and acceptor sites suggested that C domains function as additional fidelity-conferring units for the non-ribosomal peptides assemblies. Further understanding of the substrate specificity of NRPS domains is essential for studying the fundamental biochemistry of these enzymes. Moreover, knowledge concerning the substrate selectivity will be crucial for the reprogramming of NRPS assembly lines in combinatorial biosynthesis.

GrsA, the tridomain PheATE initiation module of gramicidin S synthetase, is one of the best-characterized non-ribosomal peptide synthetase (NRPS) modules (Figure 1).<sup>10–13</sup> The chemical reactions catalyzed by GrsA include adenylation of L-Phe to form L-phenylalanyl-adenosine-5'-phosphate diester (L-Phe-AMP) by the A domain, aminoacyl transfer to the HS-Ppant group in the T domain and epimerization of the covalently bound L-Phe-S-Ppant-T enzyme to D-Phe-S-Ppant-T enzyme by the E

domain. The D-Phe-S-Ppant-T enzyme will then be recognized by the condensation domain of the first module in GrsB and processed through the subsequent elongation steps to generate a pentapeptidyl-S-enzyme that is subsequently dimerized to a decapeptidyl-S-enzyme. The thioesterase domain of GrsB is proposed to dimerize and cyclize the final product gramicidin S.

Previous studies have shown that gramicidin S synthetase is able to activate a number of substrate analogues as adenylates and incorporate these compounds into gramicidin S analogue peptide products, especially at the initiation module (GrsA).<sup>14</sup> However, few details are available regarding the specificity of each domain in the PheATE initiation module, much less kinetic analysis of the rates of activation, incorporation, and epimerization of the noncognate amino acids. We report here an analysis of the substrate recognition and selection by each domain in GrsA by determining the kinetic and thermodynamic constants for individual reaction steps. For the first time, we were able to show that the E domain may also serve as a fidelity-checking element in the NRPS assembly line.

(10) Stein, T.; Kluge, B.; Vater, J.; Franke, P.; Otto, A.; Wittmann-Liebold, B. *Biochemistry* **1995**, *34*, 4633–4642.

(11) Stachelhaus, T.; Marahiel, M. A. *J. Biol. Chem.* **1995**, *270*, 6163–6169.

(12) Stachelhaus, T.; Walsh, C. T. *Biochemistry* **2000**, *39*, 5775–5787.

(13) Luo, L.; Walsh, C. T. *Biochemistry* **2001**, *40*, 5329–5337.

(14) Vater, J.; Stein, T. H. *Comprehensive Natural Products Chemistry*; Elsevier: Amsterdam, 1999; Vol. 4.

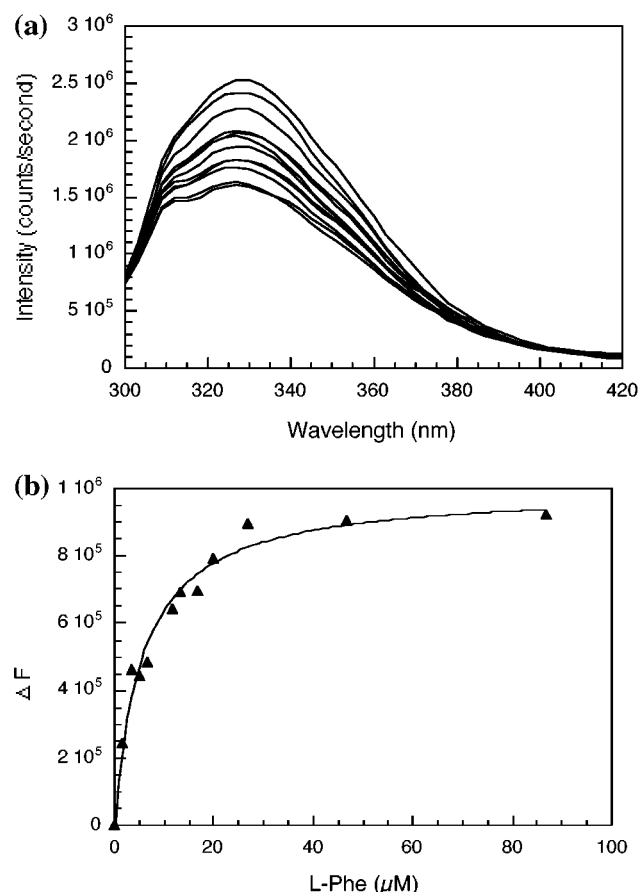


**Figure 2.** (a) Equilibrium fluorescence spectra of 0.1  $\mu\text{M}$  PheA (in 50 mM  $\text{K}^+$ Hepes, pH 7.5 at 25  $^\circ\text{C}$ ) in the presence of 0–87  $\mu\text{M}$  L-Phe (top to bottom). The spectra were scanned from 300 to 420 nm using an excitation wavelength of 280 nm. (b) The observed fluorescence change at 327 nm plotted vs [L-Phe]. The curve was fitted by eq 1.

## Results

### Determination of Binding Constants of Various Amino Acids to the Adenylation Domain by Fluorescence Titration.

To determine the dissociation constants ( $K_d$ ) of various amino acids to the adenylation domain, we employed the equilibrium fluorescence titration method. In a typical titration experiment, aliquots of ligand were added to a 3.0-mL enzyme solution (0.1  $\mu\text{M}$  PheA or 0.05  $\mu\text{M}$  apoPheATE). The solution was mixed after each aliquot of ligand was added, and the fluorescence intensity was recorded as the average of a 1-min reading. The fluorescence titration spectra of 0.1  $\mu\text{M}$  PheA measured in the presence of 0–87  $\mu\text{M}$  L-Phe are shown in Figure 2a, and the titration curve determined at 327 nm is shown in Figure 2b. At saturation, L-Phe quenches ca. 40% of the intrinsic fluorescence signal of the PheA protein. A fitting of the titration curve using eq 1 (below) gave a  $K_d$  value of 6  $\mu\text{M}$  for L-Phe to PheA (Table 1). The same  $K_d$  value (6  $\mu\text{M}$ ) was determined for L-Phe to apoPheATE (apoPheATE has no prosthetic group phosphopantetheine installed on the T domain), indicating very little effect from the other two domains, T–E, on L-Phe binding to the adenylation domain. To test whether the quenching signal we measured was correlated to amino acid binding, we used benzoic acid as a control. The titration experiment with benzoic acid gave a  $K_d$  of 83  $\mu\text{M}$ , a 14-fold increase from the 6  $\mu\text{M}$  for L-Phe, indicating that the observed fluorescence quenching was indeed a result of specific amino acid binding at the A domain active site. Dissociation constants of D-Phe, L-Tyr, L-Leu, L-Val, L-Ala, L-His, L-Arg, L-Lys, L-Asp, L-Glu, and L-Pro to PheA (listed in

**Table 1.** Dissociation Constants for Binding of Various Amino Acids to the Adenylation Domain PheA and the Adenylation Domain in ApoPheATE

amino acid	$K_d$ ( $\mu\text{M}$ )	amino acid	$K_d$ ( $\mu\text{M}$ )
L-Phe	$6 \pm 1$	L-His	$6.9 \pm 0.7$
D-Phe	$7 \pm 1$	L-Arg	$56 \pm 15$
L-Trp	na	L-Lys	$9 \pm 1$
L-Tyr	$2.0 \pm 0.3$	L-Asp	$3.3 \pm 0.7$
L-Leu	$12 \pm 2$	L-Glu	$6.6 \pm 0.7$
L-Val	$9 \pm 3$	L-Pro	$14 \pm 1$
L-Ala	$13 \pm 3$	benzoic acid	$83 \pm 10$

<sup>a</sup> Dissociation constant measured for the binding of L-Phe to apoPheATE.

Table 1) were also determined by equilibrium fluorescence titration experiments. We were unable to obtain the  $K_d$  value for L-Trp binding to PheA because of its intrinsic fluorescence signal. The similar  $K_d$  values obtained for L-Phe (6  $\mu\text{M}$ ) and D-Phe (7  $\mu\text{M}$ ) showed that the phenylalanine-binding pocket can accommodate both stereoisomers equally well, which was in agreement with the observed crystal structures of PheA containing L-Phe or D-Phe.<sup>6</sup> All other L-amino acids tested (except for L-Arg, which has a 10-fold increase in binding constant) have dissociation constants within 2–3-fold of L-Phe  $K_d$ . These results suggested that the phenylalanine-binding pocket is large enough to accommodate most other amino acids and not very sensitive to the size and charge of the side chains of the bound amino acid.

### ATP–PPi Exchange Assay for Adenylation Domain Amino Acid Selectivity.

The apoPheATE-catalyzed aminoacyl adenylation formation was first assayed by the amino acid-dependent ATP–PPi exchange assay (see Table 2). The natural substrate, L-Phe, and its stereoisomer, D-Phe, displayed similar catalytic efficiency (with a  $k_{\text{cat}}/K_m$  ratio 0.96), which is in good agreement with previous reports.<sup>11</sup> Among other proteinogenic amino acids tested, L-Trp, L-Tyr, and L-Leu showed positive signals but are 13-, 310-, and 16-fold less in catalytic efficiency ( $k_{\text{cat}}/K_m$ ), respectively. For L-Trp and L-Leu, the 13- and 16-fold decreases in catalytic efficiency resulted mostly from the 10- and 11-fold increases in  $K_m$ , while the  $k_{\text{cat}}$  decreased only slightly compared to the L-Phe reaction rate. For L-Tyr, the decrease in catalytic efficiency represents a 69-fold reduction in  $k_{\text{cat}}$  and a 4.5-fold increase in  $K_m$ . The activation of L-Val, L-Ala, and L-Pro by the A domain in apoPheATE is too weak to be detected by the ATP–PPi exchange assay.

### Amino Acid-Dependent ATP Consumption by the Adenylation Domain in ApoPheATE and HoloPheATE.

Measurement of amino acid-dependent ATP consumption was achieved by measuring the PPi release rate using an inorganic pyrophosphatase-based assay as previously described.<sup>13</sup> The steady-state kinetic constants  $k_{\text{cat}}$  and  $K_m$  measured using initial velocity techniques in conjunction with the continuous spectrophotometric assay for various amino acids allowed us to evaluate the usage of ATP in an amino acid-dependent manner and hence the ability of the A domain to form and turn over aminoacyl adenylation. As listed in Table 2, the  $k_{\text{cat}}/K_m$  values are approximately the same for L-Phe and D-Phe, and 4–10-fold lower for L-Trp, L-Tyr, and L-Leu. The spectrophotometric assay also allowed us to evaluate the L-Val- and L-Ala-dependent ATP consumptions ( $k_{\text{cat}}/K_m$ ), which are ca. 20- and 250-fold less than L-Phe-dependent ATP use. The L-Pro-dependent ATP consumption is below the detection limit. Rates of L-Phe-, L-Tyr-, and L-Ala-dependent ATP usage were also measured for holoPheATE, with the prosthetic group installed on the T domain. We observed very similar ATP consumption (evaluated

**Table 2.** Kinetic Constants for Amino Acid-Dependent ATP Hydrolysis by ApoPheATE and HoloPheATE Measured by Continuous Spectrophotometric Pyrophosphate Assay and ATP-PPi Exchange Assay

substrate	continuous spectrophotometric pyrophosphate assay (PheATE)			ATP-PPi exchange assay (apoPheATE)		
	$k_{\text{cat}}$ (min <sup>-1</sup> )	$K_{\text{m}}$ (mM)	$k_{\text{cat}}/K_{\text{m}}$ (min <sup>-1</sup> mM <sup>-1</sup> )	$k_{\text{cat}}$ (min <sup>-1</sup> )	$K_{\text{m}}$ (mM)	$k_{\text{cat}}/K_{\text{m}}$ (min <sup>-1</sup> mM <sup>-1</sup> )
L-Phe	0.06 ± 0.01 <sup>a</sup>	0.03 ± 0.01 <sup>a</sup>	2 <sup>a</sup>	690	0.07	9900
D-Phe	0.07 ± 0.02 <sup>b</sup>	0.03 ± 0.02 <sup>b</sup>	2.3 <sup>b</sup>			
D-Phe	0.06 ± 0.01 <sup>a</sup>	0.02 ± 0.008 <sup>a</sup>	3 <sup>a</sup>	720	0.07	10300
L-Trp	0.16 ± 0.02 <sup>a</sup>	0.3 ± 0.1 <sup>a</sup>	0.5 <sup>a</sup>	552	0.74	750
L-Tyr	0.17 ± 0.01 <sup>a</sup>	1.1 ± 0.1 <sup>a</sup>	0.15 <sup>a</sup>	10	0.31	32
	0.2 ± 0.02 <sup>b</sup>	1.4 ± 0.1 <sup>b</sup>	0.14 <sup>b</sup>			
L-Leu	0.18 ± 0.03 <sup>a</sup>	0.5 ± 0.2 <sup>a</sup>	0.3 <sup>a</sup>	504	0.8	630
L-Val	0.13 ± 0.02 <sup>a</sup>	1.0 ± 0.2 <sup>a</sup>	0.13 <sup>a</sup>	nd <sup>c</sup>	nd <sup>c</sup>	
L-Ala	0.03 ± 0.01 <sup>a</sup>	2.5 ± 1.0 <sup>a</sup>	0.012 <sup>a</sup>	nd <sup>c</sup>	nd <sup>c</sup>	
	0.04 ± 0.01 <sup>b</sup>	2.1 ± 0.8 <sup>b</sup>	0.019 <sup>b</sup>			
L-Pro	nd <sup>c</sup>	nd <sup>c</sup>		nd <sup>c</sup>	nd <sup>c</sup>	

<sup>a</sup> Kinetic constants measured for amino acid-dependent ATP hydrolysis by apoPheATE. <sup>b</sup> Kinetic constants measured for amino acid-dependent ATP hydrolysis by holoPheATE. <sup>c</sup> nd, not detectable.

by  $k_{\text{cat}}/K_{\text{m}}$  by apoPheATE and holoPheATE for all three amino acids tested. For holoPheATE-catalyzed aminoacyl-adenylate formation, the HS-pantetheine arm attached to the T domain can reach the A domain active site and capture the amino acyl group from aminoacyl-adenylate. Without the presence of a thioesterase domain, the loaded pantetheinyl group will hydrolyze only at a very slow rate by the water solvent. Hence, the ATP consumption for holoPheATE after the aminoacyl group transfer was essentially the same as that for apoPheATE.

**Aminoacyl-AMP Formation by ApoPheATE under Single-Turnover Reaction Conditions.** Single-turnover analyses were carried out to determine the transient kinetic rates of various aminoacyl-AMP formations within the active site of the apoPheATE A domain. The apoPheATE enzyme (35  $\mu\text{M}$ ) was acid-quenched after exposure to ATP (4 mM) and radiolabeled amino acid substrate (6  $\mu\text{M}$ ) for specified periods of time using a rapid-quench apparatus. At a final concentration of 35  $\mu\text{M}$  enzyme and 6  $\mu\text{M}$  amino acid, we calculated that 74–84% of free amino acids will be enzyme-bound according to the  $K_{\text{d}}$  values measured by fluorescence titration, validating the single-turnover status of the reactions. Previous studies showed that the catalytic step is rate-limiting for L-Phe and apoPheATE single-turnover reactions.<sup>13</sup> To demonstrate that the observed rate constants reflect the rate of the catalytic step instead of substrate binding for the noncognate amino acid substrates, we carried out single time point reactions at double the final apoPheATE (66  $\mu\text{M}$ ) concentration. The reactions were quenched at the half-life ( $t_{1/2}$ ) of each reaction. The increase of the aminoacyl-AMP formations was less than 20% for all four noncognate amino acids compared to the reactions carried out with 35  $\mu\text{M}$  final apoPheATE, indicating that the rates measured were indeed the rates of the chemical step. The profiles for single-turnover reactions of apoPheATE with L-Phe, D-Phe, L-Trp, L-Tyr, and L-Leu are shown in Figure 3, and the rate data fitted to a first-order reaction kinetic model (eq 2, below) using the program DYNAFIT are listed in Table 3. The rate constants for aminoacyl-AMP formation were reduced 0.7-fold for D-Phe-AMP, 2.5-fold for L-Trp-AMP, 910-fold for L-Tyr-AMP, and 20-fold for L-Leu-AMP compared to that of L-Phe-AMP. Meanwhile, the reverse reaction rates were unchanged for L-Trp and L-Leu, increased 2.4-fold for D-Phe, and decreased 45-fold for L-Tyr. At the completion of the single-turnover reaction, the ratio of aminoacyl-AMP and the starting amino acid (observed internal equilibrium constant) decreased from 2 for the L-Phe reaction to 0.6 for D-Phe, 0.8 for L-Trp, 0.1 for L-Tyr, and 0.1 for L-Leu. These reductions in internal equilib-

rium constants reflect a decrease in the ability of the PheA domain to stabilize the different aminoacyl-adenylate intermediates.

**Covalent Loading of Amino Acids to the T Domain of the HoloPheATE.** To inquire whether the activated noncognate amino acids (in the form of aminoacyl-AMP) can be recognized and loaded to the downstream T domain, the transfer of aminoacyl groups to the T domain was examined in holoPheATE-catalyzed reactions. The assay entailed detecting covalently radiolabeled holoPheATE by TCA precipitation under single-turnover conditions (35  $\mu\text{M}$  holoPheATE + 6  $\mu\text{M}$  radioactive amino acid). The reactions were TCA quenched after 40 min to ensure the completion of the loading. As shown in Figure 4, the percentage of thiolation varied from 88% for the L-Phe reaction to 0.1% for the L-Gly reaction. Among the 17 amino acids tested, L-Phe, D-Phe, L-Trp, L-Tyr, and L-Leu showed significant loading on the T domain.

**Single-Turnover Profiles for HoloPheATE-Catalyzed Adenylation, Thiolation, and Epimerization Reactions for Various Amino Acid Ligands.** With the aminoacyl-adenylation by the A domain and thiolation of the T domain demonstrated, the epimerization of the covalently tethered noncognate amino acids and the kinetic profiles for all three steps by holoPheATE were next examined. Single-turnover rapid quench analysis was utilized to evaluate the three sequential reaction steps, adenylation, thiolation, and epimerization by the A, T, and E domains, respectively. This technique allowed us to evaluate the rates of the three reactions for different amino acids catalyzed by holoPheATE. Reactions were carried out by reacting holoPheATE (35  $\mu\text{M}$ ) with radiolabeled amino acid (6  $\mu\text{M}$ ) in the presence of saturating ATP and  $\text{Mg}^{2+}$ . The reactions were acid-quenched at varying times, and the radioactive species in the supernatant (amino acid and aminoacyl-AMP) were separated from those in the protein pellet (L-a.a.-S-Ppant-enzyme and D-a.a.-S-Ppant-enzyme). The supernatant and the hydrolyzed products of the pellet were then analyzed by cellulose TLC and chiral TLC as previously described.<sup>13</sup> The time courses of single-turnover reactions were globally fitted to the kinetic model (eq 3, below) as previously described using the program DYNAFIT (Figure 5).<sup>13</sup> As shown in Figure 5, there are several noticeable differences among the reactions: (1) The overall reaction rates for L-Phe and D-Phe are at least 2 orders of magnitude faster than those of L-Trp, L-Tyr, and L-Leu. (2) The accumulation of aminoacyl-AMP reaches 20% of the starting amino acid for L-Phe and D-Phe reactions, while the accumulation of aminoacyl-AMP for L-Trp, L-Tyr, and L-Leu reactions is at most 3%. (3)

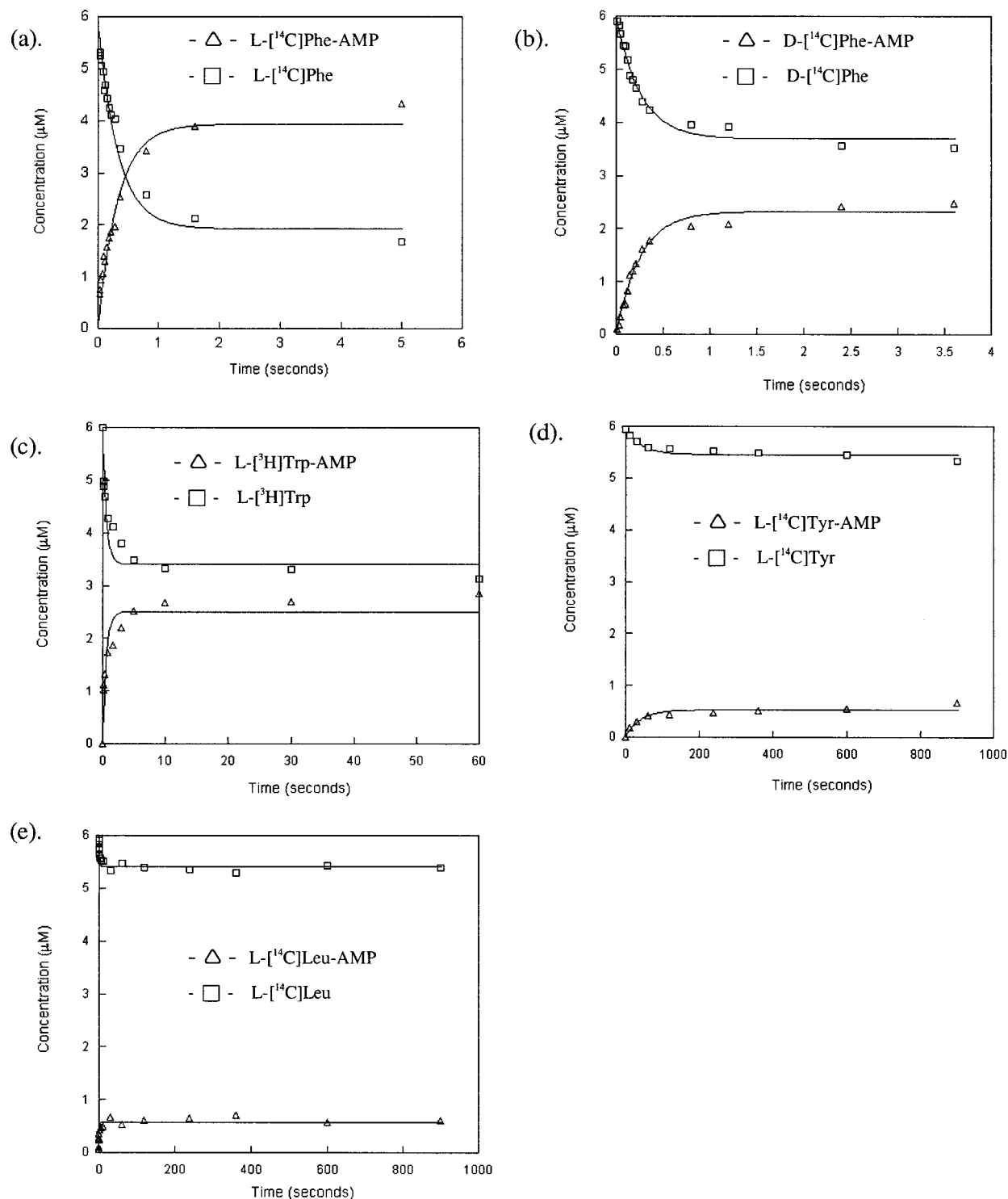


**Figure 3.** Time courses for the single-turnover reactions of 35  $\mu\text{M}$  apoPheATE enzyme with 6  $\mu\text{M}$  radiolabeled amino acid, 5 mM  $\text{MgCl}_2$ , 4 mM ATP, and 0.5 mM TCEP in 50 mM  $\text{K}^+\text{Hepes}$  (pH 7.5). (a) L- $^{14}\text{C}$ ]Phe ( $\square$ ) and L- $^{14}\text{C}$ ]Phe-AMP ( $\Delta$ ); (b) D- $^{14}\text{C}$ ]Phe ( $\square$ ) and D- $^{14}\text{C}$ ]Phe-AMP ( $\Delta$ ); (c) L- $^3\text{H}$ ]Trp ( $\square$ ) and L- $^3\text{H}$ ]Trp-AMP ( $\Delta$ ); (d) L- $^{14}\text{C}$ ]Tyr ( $\square$ ) and L- $^{14}\text{C}$ ]Tyr-AMP ( $\Delta$ ); and (e) L- $^{14}\text{C}$ ]Leu ( $\square$ ) and L- $^{14}\text{C}$ ]Leu-AMP ( $\Delta$ ) are shown with progress curves fitted by DYNAFIT.

For both L-Phe and D-Phe reactions, the D-Phe-S-Ppant-enzyme is preferred as the product at equilibrium with a 60/40 split of D-Phe-/L-Phe-S-Ppant-enzyme. In contrast, L-a.a.-S-Ppant-enzyme is the dominant product for L-Trp, L-Tyr, and L-Leu reactions at equilibrium. The ratio of D-a.a.-S-Ppant-enzyme/L-a.a.-S-Ppant-enzyme is ca. 0.7 for L-Trp, L-Tyr, and L-Leu reactions. The microscopic rate constants and the apparent internal equilibrium constants for individual reaction steps catalyzed by holoPheATE starting from five different amino

acids are listed in Table 4. The rates for the L-Phe and D-Phe reactions were largely comparable. For L-Trp, L-Tyr, and L-Leu reactions, these amino acids were converted to enzyme-bound aminoacyl-AMPs at rates 16-, 1200-, and 12-fold slower than L-Phe. The apparent internal equilibrium constants  $K_1^{\text{app}}$  (calculated from  $k_1/k_{-1}$ ) listed in Table 4 showed that, thermodynamically, the [holoPheATE·L-a.a.-AMP· $\text{Mg}^{2+}$ ·PPi] complex was most stable for L-Phe-AMP and least stable for L-Leu-AMP bound at the active site. For the thiolation step, the rates for

**Table 3.** Rate Constants for Aminoacyl-AMP Formation Catalyzed by ApoPheAT

amino acid	$K_{\text{eq}}^{\text{app}^b}$	$k_1$ ( $\text{s}^{-1}$ )	$k_{-1}$ ( $\text{s}^{-1}$ )
L-Phe	2	$2.0 \pm 0.1$	$1.0 \pm 0.1$
D-Phe	0.6	$1.5 \pm 0.06$	$2.4 \pm 0.1$
L-Trp	0.8	$0.8 \pm 0.1$	$1.0 \pm 0.2$
L-Tyr	0.1	$0.0022 \pm 0.0004$	$0.022 \pm 0.004$
L-Leu	0.1	$0.1 \pm 0.02$	$1.0 \pm 0.2$
L-Pro		nd <sup>a</sup>	nd <sup>a</sup>

<sup>a</sup> Formation of L-Pro-AMP not detectable. <sup>b</sup> Apparent internal equilibrium constant = [aminoacyl-AMP]/[amino acid] measured from the ratio of the two species at equilibrium.

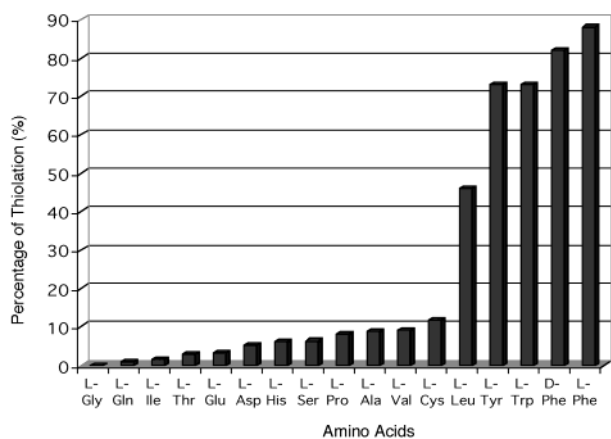


**Figure 4.** Percent of radiolabeled amino acid loaded to holoPheATE under single-turnover conditions (35  $\mu\text{M}$  apoPheATE enzyme with 6  $\mu\text{M}$  radiolabeled amino acid, 5 mM  $\text{MgCl}_2$ , 4 mM ATP, and 0.5 mM TCEP in 50 mM  $\text{K}^+\text{Hepes}$  (pH 7.5) incubated for 40 min; 100% loading corresponds to 6  $\mu\text{M}$  amino acid loaded holoPheATE).

L-Trp, L-Tyr, and L-Leu reactions were down 38-, 1-, and 23-fold, respectively. The  $K_2^{\text{app}}$  values revealed that L-aminoacyl-S-Pant-enzymes were more favorable thermodynamically than enzyme-aminoacyl-AMP complexes. This preference was more evident for L-Leu and L-Trp (with  $K_2^{\text{app}} = 30$  and 34, respectively) due to the poor stability of their enzyme-aminoacyl-AMP complexes. The most interesting changes were observed in the rates for the final step, epimerization of the L-aminoacyl-S-Pant-enzyme to D-aminoacyl-S-Pant-enzyme intermediate. Three noncognate amino acids showed rates reduced by 245-, 300-, and 540-fold ( $0.005$ ,  $0.009$ , and  $0.011 \text{ s}^{-1}$  for L-Leu, L-Tyr, and L-Trp reactions vs  $2.7 \text{ s}^{-1}$  for L-Phe reaction). Additionally, the  $K_3^{\text{app}}$  values (ca. 0.7 for all three amino acids) displayed an obvious preference of L-aminoacyl-S-Pant-enzyme at equilibrium. In contrast, the D-Phe-S-Pant-enzyme form was preferred regardless of whether the starting amino acid was L-Phe or D-Phe.

**Free Energy Profiles for HoloPheATE Catalysis.** The microscopic rate constants and thermodynamic equilibrium constants derived from DYNAFIT fitting were used to construct energy profiles for holoPheATE-catalyzed three-step reactions under single-turnover conditions (Figure 6). The enzyme-substrate complex (ES) was assigned as ground state with free energy of 0 kcal/mol. The free energy profiles showed the kinetic and thermodynamic bases for PheATE substrate selection. In the adenylation step, the energy barrier for the transition state could be much higher for noncognate amino acids such as Tyr so that the reaction would be substantially slowed. On the other hand, the bound L-aminoacyl-AMP could be a very high energy intermediate so that the reverse reaction will be predominant (as for L-Leu reaction). The energy profiles also demonstrated that the E domain reaction exerts another higher

energy barrier for noncognate amino acid substrates, suggesting its function as a significant gatekeeper in the NRPS assembly line.

**Assay of Epimerization Activity in ApoPheATE Using Aminoacyl-S-Pantetheine Surrogates.** To further study the epimerization activity of the E domain in GrsA, a series of aminoacyl-S-pantetheines were synthesized as small-molecule probes. Aminoacyl-S-pantetheines were first tested for their stability and displayed half-lives around 90 min (unpublished data) at pH 7.5 (data not shown). Since the incubation times for the enzymatic incubations performed were 30 min, the stabilities of aminoacyl-S-pantetheines are sufficient for the epimerization activity assay with apoPheATE. The kinetic analyses were performed on six aminoacyl-S-pantetheines under steady-state conditions. The thioester linkage to the pantetheine portion of the molecule was then hydrolyzed using 0.1 N potassium hydroxide to generate free amino acids. Control reactions under the same condition showed that the workup did not cause any epimerization. The free amino acids were then analyzed by chiral HPLC. The steady-state kinetic constants ( $k_{\text{cat}}$  and  $K_m$ ) obtained are listed in Table 5. All aminoacyl-S-pantetheines tested exhibited epimerization activity. The rates of epimerization for different aminoacyl-S-pantetheine analogues varied 12-fold over a range from 0.4 to 4.7  $\text{min}^{-1}$ , with the largest difference seen between the L-Phe-pant and D-Phe-pant reactions. The  $K_m$  values measured for a.a.-pant were in the millimolar range, suggesting a very weak binding of these small molecule surrogates. The overall catalytic efficiencies for those aminoacyl-S-pantetheine derivatives were surprisingly close. We surmised that the discrepancy between the *in cis* single-turnover analysis and small-molecule surrogates studies indicated that the protein scaffold of the T domain may play an important role for substrate recognition and selection in E domain catalysis.

## Discussion

The sequence of non-ribosomal peptide natural products is determined not by mRNA templates but by the order and identity of catalytic and carrier protein domains in the modules of non-ribosomal peptide assembly lines. The use of aminoacyl-AMP intermediates followed by covalent tethering of the activated aminoacyl groups as aminoacyl-S-enzymes on phosphopantetheinyl arms of thiolation domains by paired A-T domains mirrors the strategy of aminoacyl-tRNA synthetases in ribosomal peptide synthesis, where aminoacyl-AMP formations are followed by covalent connection of the selected aminoacyl group to the 3'-end of the cognate tRNA.<sup>15</sup> In the aminoacyl-tRNA synthetases, the translational fidelity is ensured by editing (proofreading) of noncognate aminoacyl intermediates at either the aminoacyl-AMP (pretransfer editing) or the aminoacyl-tRNA (posttransfer editing) level.<sup>15-18</sup> By comparison, it has not been known if the A domains of NRPS catalysts have comparably robust fidelity and editing functions. Indeed, it is known that noncognate proteinogenic amino acids can be incorporated to a few percent abundance in such peptides as cyclosporins and gramicidin S,<sup>14,19</sup> including residue one, specified by the PheATE tridomain initiation module, the GrsA subunit studied here.

(15) Ibba, M.; Soll, D. *Annu. Rev. Biochem.* **2000**, *69*, 617-650.

(16) Fersht, A. R. *Biochemistry* **1977**, *16*, 1025-1030.

(17) Fersht, A. R.; Dingwall, C. *Biochemistry* **1979**, *18*, 1238-1245.

(18) Nureki, O.; Vassilyev, D. G.; Tateno, M.; Shimada, A.; Nakama, T.; Fukai, S.; Konno, M.; Hendrickson, T. L.; Schimmel, P.; Yokoyama, S. *Science* **1998**, *280*, 578-582.

(19) Kleinkauf, H.; von Doehren, H. *Prog. Drug Res.* **1990**, *34*, 287-317.

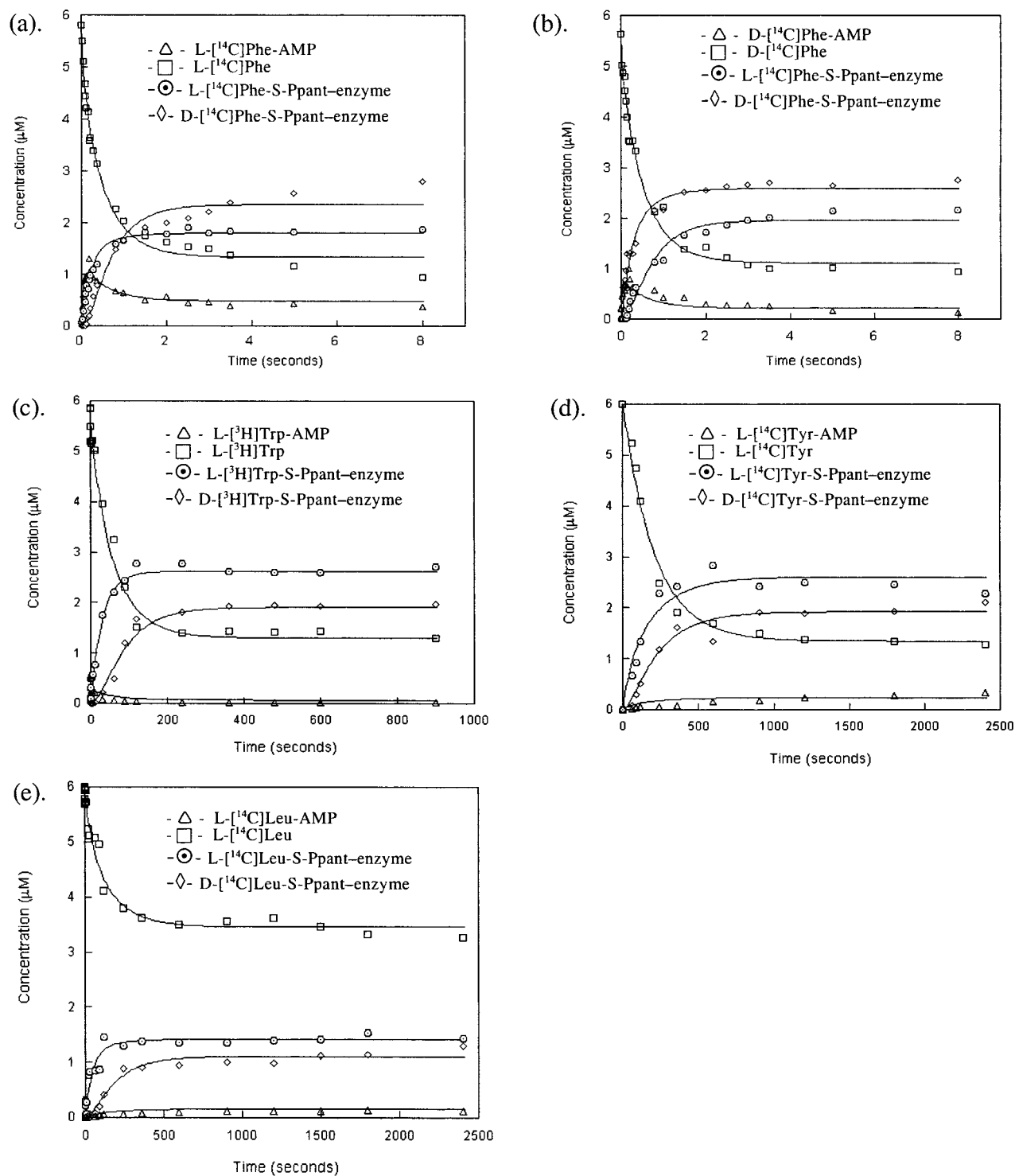


**Figure 5.** Time courses for the single-turnover reactions of 35  $\mu\text{M}$  holoPheATE enzyme with 6  $\mu\text{M}$  radiolabeled amino acid, 5 mM  $\text{MgCl}_2$ , 4 mM ATP, and 0.5 mM TCEP in 50 mM  $\text{K}^+\text{Hepes}$  (pH 7.5). (a) L- $^{14}\text{C}$ Phe ( $\square$ ), L- $^{14}\text{C}$ Phe-AMP ( $\triangle$ ), D- $^{14}\text{C}$ Phe-S-Ppant-enzyme ( $\diamond$ ), and L- $^{14}\text{C}$ Phe-S-Ppant-enzyme ( $\odot$ ); (b) D- $^{14}\text{C}$ Phe ( $\square$ ), D- $^{14}\text{C}$ Phe-AMP ( $\triangle$ ), D- $^{14}\text{C}$ Phe-S-Ppant-enzyme ( $\diamond$ ), and L- $^{14}\text{C}$ Phe-S-Ppant-enzyme ( $\odot$ ); (c) L- $^3\text{H}$ Trp ( $\square$ ), L- $^3\text{H}$ Trp-AMP ( $\triangle$ ), D- $^3\text{H}$ Trp-S-Ppant-enzyme ( $\diamond$ ), and L- $^3\text{H}$ Trp-S-Ppant-enzyme ( $\odot$ ); (d) L- $^{14}\text{C}$ Tyr ( $\square$ ), L- $^{14}\text{C}$ Tyr-AMP ( $\triangle$ ), D- $^{14}\text{C}$ Tyr-S-Ppant-enzyme ( $\diamond$ ), and L- $^{14}\text{C}$ Tyr-S-Ppant-enzyme ( $\odot$ ); and (e) L- $^{14}\text{C}$ Leu ( $\square$ ), L- $^{14}\text{C}$ Leu-AMP ( $\triangle$ ), D- $^{14}\text{C}$ Leu-S-Ppant-enzyme ( $\diamond$ ), and L- $^{14}\text{C}$ Leu-S-Ppant-enzyme ( $\odot$ ) are shown with progress curves fitted by DYNAFIT.

Our recent transient kinetic analysis of the three intermediates, L-Phe-AMP, L-Phe-S-enzyme, and D-Phe-S-enzyme, produced by PheATE,<sup>13</sup> set the stage for analysis of discrimination by this NRPS chain initiation module against other proteinogenic amino acids. From initial evaluation of endpoint assays for covalent loading of radioactive amino acids as the radiolabeled

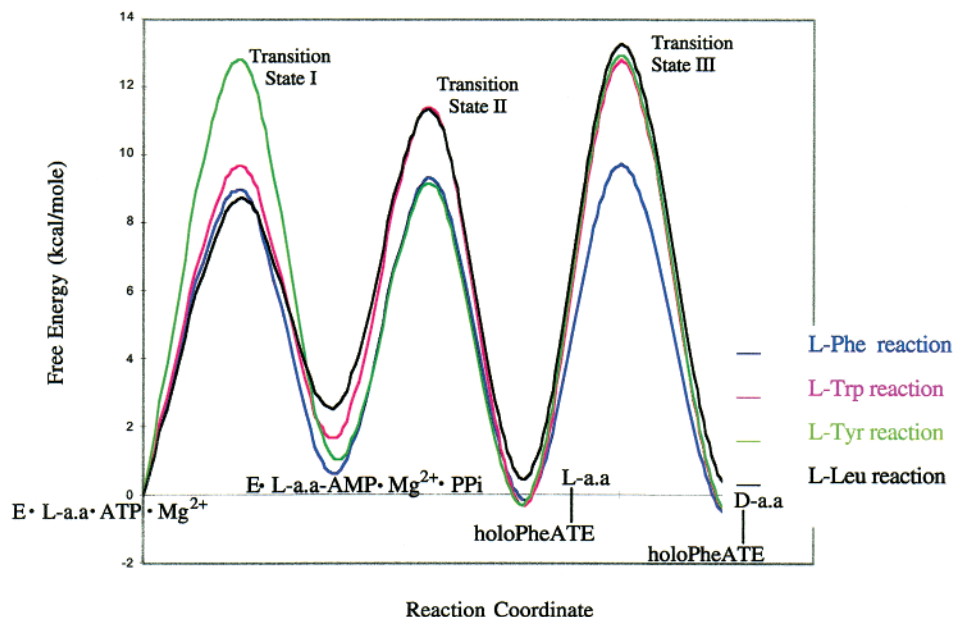
aminoacyl-S-T domain intermediates, we focused more closely on L-Tyr, L-Trp, and L-Leu as analogues that can compete with L-Phe.

In the initial binding step of L-amino acids to the A domain active site, fluorescence quenching analysis indicated that both L-Phe and D-Phe bound equally well ( $K_d$  at 6 and 7  $\mu\text{M}$ ,

**Table 4.** Rate Constants and Apparent Internal Equilibrium Constants for Individual Reaction Steps Catalyzed by holoPheATE Using Different Amino Acid as Starting Substrate under Single-Turnover Conditions (See Experimental Procedures for Details)<sup>a</sup>

	$k_1$ (s <sup>-1</sup> )	$k_{-1}$ (s <sup>-1</sup> )	$k_2$ (s <sup>-1</sup> )	$k_{-2}$ (s <sup>-1</sup> )	$k_3$ (s <sup>-1</sup> )	$k_{-3}$ (s <sup>-1</sup> )
holoPheATE + L-[ <sup>14</sup> C]Phe	4.7 ± 0.5 $K_1^{\text{app}} = 0.36$	13 ± 2	7.9 ± 0.6 $K_2^{\text{app}} = 3.8$	2.1 ± 0.3	2.7 ± 0.4 $K_3^{\text{app}} = 1.3$	2.1 ± 0.3
holoPheATE + D-[ <sup>14</sup> C]Phe	8 ± 2 $K_1^{\text{app}} = 0.21$	39 ± 14	11 ± 1 $K_2^{\text{app}} = 11$	1.0 ± 0.2	1.8 ± 0.4 $K_3^{\text{app}} = 0.72$	2.5 ± 0.6
holoPheATE + L-[ <sup>3</sup> H]Trp	0.3 $K_1^{\text{app}} = 0.06$	5.3	0.3 $K_2^{\text{app}} = 30$	0.01	0.011 $K_3^{\text{app}} = 0.69$	0.016
holoPheATE + L-[ <sup>14</sup> C]Tyr	0.004 $K_1^{\text{app}} = 0.17$	0.024	11 $K_2^{\text{app}} = 9$	1.2	0.009 $K_3^{\text{app}} = 0.75$	0.012
holoPheATE + L-[ <sup>14</sup> C]Leu	0.39 $K_1^{\text{app}} = 0.014$	28	0.34 $K_2^{\text{app}} = 34$	0.01	0.005 ± 0.001 $K_3^{\text{app}} = 0.71$	0.007 ± 0.002

<sup>a</sup> The apparent internal equilibrium constants were calculated from the ratio of microscopic rate constants.

**Figure 6.** Reaction free energy profiles for holoPheATE-catalyzed adenylation, thiolation, and epimerization reactions using L-Phe, L-Trp, L-Tyr, and L-Leu as the starting amino acid substrate. The concentrations of the reaction components were described in the Experimental Procedures. The free energy change and the apparent free energies of activation for each step were calculated from the constants in Table 4. The free energy profile for the L-Phe reaction is in blue, L-Trp in magenta, L-Tyr in green, and L-Leu in black.**Table 5.** Rate Constants for Epimerization Reaction by E Domain in the PheATE Module Using Various a.a.-S-pant Analogues as Substrate

	$k_{\text{cat}}$ (min <sup>-1</sup> )	$K_m$ (mM)	$k_{\text{cat}}/K_m$ (min <sup>-1</sup> /mM)
L-Phe-pantetheine	4.7 ± 0.9	10 ± 3	0.5
D-Phe-pantetheine	0.4 ± 0.03	2.1 ± 0.4	0.2
L-Tyr-pantetheine	1.7 ± 0.1	5.6 ± 0.9	0.3
L-Thr-pantetheine	1.1 ± 0.7	1.5 ± 0.3	0.7
L-Leu-pantetheine	3.1 ± 0.3	6.1 ± 1.4	0.5
N-acetyl-L-Phe-pantetheine	2.8 ± 0.3	2.0 ± 0.8	1.4

respectively) but, surprisingly, other L-amino acids bind almost equally well ( $K_d$  within 2–3-fold), so there is no substantial energy difference in formation of the collisional enzyme–substrate complex. Discrimination starts with the first chemical step, where the A domain catalyzes attack of the carboxylate of the bound L-amino acid on the  $\alpha$ -phosphate of ATP to yield the bound aminoacyl-AMP. Presumably, the noncognate amino acid could encounter a much higher energy barrier at the transition state and/or form a higher energy and less stable aminoacyl-AMP intermediate.

Of the three assays of A domain function, amino acid-driven [<sup>32</sup>P]-PPi-ATP exchange, amino acid-dependent ATPase action,

and rapid quench studies under single-turnover conditions, the latter is the most direct and accurate measurement of aminoacyl-AMP formation. In contrast, the rates determined by amino acid-driven [<sup>32</sup>P]-PPi-ATP exchange assay included both forward and reverse reaction steps of [<sup>32</sup>P]-PPi with aminoacyl-AMP during the exchange process. This assay measured the incorporation of labeled pyrophosphate (PPi) in ATP and has been used as a standard activity test for aminoacyl-tRNA synthetase and other adenylate-forming enzymes.<sup>16,17</sup> Mechanistically, it is the reverse reaction of amino acid activation, and thus the rate measured by this assay should include not only aminoacyl-AMP formation but also the phosphorylation of the AMP by pyrophosphate. The ATPase catalytic turnover assay, which measures the slow steady-state, multiple-turnover rate due to adventitious release and loss of aminoacyl-AMP,<sup>13</sup> is limited by very slow off-rates of the tightly bound aminoacyl-AMP and hence not an accurate measurement of aminoacyl-AMP formation. Nevertheless, all three different assays of the A domain function in apoPheATE showed that detectable amounts of D-Phe-AMP, L-Trp-AMP, L-Tyr-AMP, and L-Leu-AMP were formed and bound by the enzyme at the active site. The single-turnover profiles for the formations of four noncognate aminoacyl-AMP intermediates (D-Phe-AMP, L-Trp-AMP, L-Tyr-AMP, and L-Leu-AMP) dis-

played no hydrolytic editing of the misactivated aminoacyl-AMPs by enzyme as all misactivated aminoacyl-AMPs plateaued after equilibrium was reached. In addition, no extra ATP consumption was observed in the coupled ATPase activity assay, and only moderate PPI exchange was seen in [<sup>32</sup>P]-PPI-ATP exchange assay when noncognate amino acids were charged to AMP. Thus, there is no indication of pretransfer editing of misactivated aminoacyl-AMP by the GrsA A domain. The possibility of posttransfer editing (hydrolytic proofreading of the misacylated Ppant arm of the T domain) was explored by coupled ATPase activity assay of holoPheATE activation of noncognate amino acids. The close match in ATP usage by apoPheATE and holoPheATE was observed for both cognate and noncognate amino acids, showing no evidence for post-transfer editing. The possibility of posttransfer was further eliminated by single-turnover profiles of holoPheATE-catalyzed noncognate amino acid reaction, where no hydrolysis of mischarged HS-Ppant-Ts was observed. For the PheATE tridomain initiation module, once the ligand is bound to the A domain and transferred to the holo-T domain, the competition of the ligand with other amino acids is removed. Without A domain editing, any slow reaction steps downstream such as condensation or epimerization reactions could be very “energy expensive” for the host microorganism. Of interest, next to almost all bacterial NRPS operons, including that of gramicidin S synthetase, distinct genes encoding a thioesterase-like protein have been detected. Studies have shown that these external thioesterase domains are directly involved in NRP biosynthesis, and there is speculation of involvement in editing functions.<sup>20,21</sup> The NRPS assembly lines may have evolved a distinct editing mechanism, relying not on internal A domains but an external thioesterase domain to liberate the mischarged phosphopantetheinyl arms.<sup>20</sup>

For holoPheATE single-turnover reactions, the discrimination against L-Tyr-AMP vs L-Phe-AMP formation was robust (1/2000), while against L-Trp-AMP (1/20) and L-Leu-AMP (1/12), the selectivity was down 2 of the 3 orders of magnitude. The second step of A domain catalysis is transfer of the activated aminoacyl moiety to the HS-pantetheinyl arm of the paired thiolation domain to install it as the covalent aminoacyl-S-enzyme intermediate. In this second half-reaction of the A domain of holoPheATE, there was no discrimination in the rate of L-tyrosyl vs L-phenylalanyl transfer (1/1), while the L-tryptophanyl transfer rate was at 1/38 and that of L-leucyl capture as the thioester at 1/23. The net selectivity for the two steps of A domain catalysis were 1/1200 for L-Tyr, 1/608 for L-Trp, and 1/245 for L-Leu.

The epimerization domain, catalyzing the third step of the initiation module reaction, converts L-Phe-S-enzyme into a 2/1 mix of D-Phe-/L-Phe-S-enzyme. The E domain turns out to be at least as robust a selectivity filter as the A domain, with 1/300 for L-Tyr-S-enzyme epimerization compared to the Phe system, 1/545 for L-Trp-, and 1/245 for the L-Leu-S-T domain as epimerization substrate. The net kinetic selectivity in the three-step discrimination by the PheATE module is 1/360 000 for L-Tyr, 1/150 000 for L-Trp, and 1/150 000 for L-Leu. If this selectivity filter function is generalizable to E domains in other NRPS modules, e.g., in elongation modules, this will condition the flux in combinatorial biosynthetic schemes, making peptides with D-amino acid constituents.

To evaluate the aminoacyl/peptidyl group specificity of E

domains embedded in ATE or CATE modules requires the in situ generation of the aminoacyl-/peptidyl-S-T domain intramolecular acyl-S-enzyme substrates. To simplify the analysis, we tested several low-molecular-weight aminoacyl-S-pantetheinyl thioesters as surrogate substrates for E domain catalysis. Table 5 shows that the full-length pantetheinyl arm allowed recognition by the E domain in the PheATE module. Five low-molecular-weight aminoacyl-S-pantetheines showed about equivalent catalytic efficiency, which is distinct from the situation where the aminoacyl-S-pantetheinyl arm is presented on the 10-kDa T domain protein scaffold *in cis*. The  $k_{\text{cat}}$  values of 1–4 min<sup>-1</sup> for the low-molecular-weight thioesters are close to the values of 0.3–0.6 min<sup>-1</sup> for Tyr- and Leu-S-enzyme (Table 4) under single-turnover conditions, while the L-Phe-S-enzyme is about 30-fold faster than L-Phe-pant for epimerase processing. It may be that most of the selectivity of the E domain is provided by  $K_m$  for the intramolecular aminoacyl-S-T domain epimerization substrate.

If the 10<sup>5</sup>-fold selectivity of the PheATE domain turns out to be prototypical for NRPS modules, the question of how other proteinogenic amino acids are incorporated at observed low frequencies arises. For initiation modules that start non-ribosomal peptide chains with L- rather than D-amino acids, two-domain A-T modules may only give 10<sup>2</sup>–10<sup>3</sup>-fold selectivity, as shown here for the two A-T steps. Elongation modules that incorporate L-amino acids have C-A-T domains, and the kinetic selectivity of C domains for upstream peptidyl chain donors is not yet clear. The PheATE module of GrsA interfaces *in trans* with the four-module GrsB subunit,<sup>22,23</sup> with the C domain of the Pro<sub>2</sub> CAT module generating the D-Phe<sub>1</sub>-L-Pro<sub>2</sub>-S-T<sub>2</sub> acyl enzyme on GrsB. This is estimated to occur with rates of 1–2 min<sup>-1</sup><sup>7,23</sup> and is slow relative to the catalytic steps of the PheATE module with its cognate amino acid.<sup>13</sup> The kinetic discrimination against generation of the noncognate D-aminoacyl-S-T intermediates in PheATE will be suppressed by slow C domain action in the dipeptidyl-S-T<sub>2</sub>-forming step, allowing fractional buildup of the noncognate D-aminoacyl-S-enzyme forms on PheATE.

In sum, despite the lack of evidence of any kinetic editing by the A domain, the three-domain PheATE module of the GrsA subunit achieves 10<sup>5</sup>-fold selectivity for its cognate L-Phe, and the epimerase domain is a major contributor to the kinetic basis of selectivity.

## Experimental Procedures

**General.** ApoPheATE protein and the adenylation domain of the PheATE module (PheA) were overexpressed and purified as previously described.<sup>11,12</sup> The proteins were obtained in a homogeneous state as judged by SDS-PAGE analysis and dialyzed into 50 mM K<sup>+</sup>Hepes buffer (pH 7.5, 1 mM tris(2-carboxyethyl)phosphine (TCEP)). Post-translational modification of apoPheATE was achieved by incubation with CoASH and *Bacillus subtilis* Ppant transferase Sfp.<sup>24,25</sup> Reaction mixtures in assay buffer contained 70 μM apo enzyme, 250 μM CoASH, and 50 nM Sfp and were incubated for 60 min at 37 °C. Equilibrium fluorescence measurements were carried out at 30 °C using a PTI fluorescence system (MD-5020 motor driver, LPS-220B lamp power supply, 814 photomultiplier detection system). Radiolabeled amino acids (a.a.) 1-[<sup>14</sup>C]Phe (450 mCi/mmol), D-[<sup>14</sup>C]Phe (56 mCi/mmol), L-[<sup>14</sup>C]-

(22) Vater, J.; Schlumbohm, W.; Palacz, Z.; Salsnikow, J.; Gadow, A.; Kleinkauf, H. *Eur. J. Biochem.* **1987**, *163*, 297–302.

(23) Stachelhaus, T.; Mootz, H. D.; Bergendahl, V.; Marahiel, M. A. *J. Biol. Chem.* **1998**, *273*, 22773–22781.

(24) Lambalot, R. H.; Gehring, A. M.; Flugel, R. S.; Zuber, P.; LaCelle, M.; Marahiel, M. A.; Reid, R.; Khosla, C.; Walsh, C. T. *Chem. Biol.* **1996**, *3*, 923–936.

(25) Quadri, L. E. N.; Weinreb, P. H.; Lei, M.; Nakano, M. M.; Zuber, P.; Walsh, C. T. *Biochemistry* **1998**, *37*, 1585–1595.

(20) Heathcote, M. L.; Staunton, J.; Leadlay, P. F. *Chem. Biol.* **2001**, *8*, 207–220.

(21) Schneider, A.; Marahiel, M. A. *Arch. Microbiol.* **1998**, *169*, 404–410.

Tyr (495 mCi/mmol), L-[<sup>14</sup>C]Leu (308 mCi/mmol), L-[<sup>14</sup>C]Ile (342 mCi/mmol), L-[<sup>14</sup>C]Ala (162 mCi/mmol), L-[<sup>14</sup>C]Gly (114 mCi/mmol), L-[<sup>14</sup>C]Pro (246 mCi/mmol), L-[<sup>14</sup>C]Ser (120 mCi/mmol), L-[<sup>14</sup>C]Thr (231.1 mCi/mmol), L-[<sup>14</sup>C]Asp (207.2 mCi/mmol), L-[<sup>14</sup>C]Glu (282 mCi/mmol), L-[<sup>14</sup>C]Gln (266 mCi/mmol), L-[<sup>14</sup>C]Cys (100 mCi/mmol), L-[<sup>3</sup>H]His (50.4 Ci/mmol), L-[<sup>3</sup>H]Trp (21.2 Ci/mmol), and L-[<sup>3</sup>H]Val (60 Ci/mmol) were purchased from NEN or Amersham Pharmacia Biotech. Sodium [<sup>32</sup>P]-pyrophosphate (534 μM, 19 Ci/mmol) was purchased from NEN. Phosphorimages of TLC plates were obtained after 12–96-h exposure to BAS-MS2040 or BAS-TR2040 image plates and read by a Bio-Imaging Analyzer BAS1000 (Fuji). The synthesis of aminoacyl-pantetheine (a.a.-pant) analogues will be described in a separate manuscript. <sup>1</sup>H NMR spectra were recorded on a Varian M200 spectrometer at 200 MHz. MALDI-TOF mass spectrometry was carried out using a Perseptive Biosystems Voyager-DESTR mass spectrometer. Analytical HPLC was carried out on a Beckman Gold Nouveau system.

**Determination of Amino Acid Binding Constants by Fluorescence Titration.** All fluorescence titration experiments were carried out using a PTI fluorescence system. The excitation wavelength was 280 nm (295 nm for L-Tyr), and the emission spectra were recorded in the range of 300–420 nm for 3-mL solutions containing 0.1 μM PheA (or 0.05 μM PheATE) and 0–200 μM amino acid ligand in 50 mM K<sup>+</sup>Hepes buffer (pH 7.5). The amino acid ligands L-Phe, D-Phe, L-Tyr, L-Leu, L-Val, L-Ala, L-Pro, L-Arg, L-Lys, L-Glu, L-His, and L-Asp were titrated to PheA, and L-Phe was titrated to PheATE to obtain the apparent dissociation constants. Benzoic acid was titrated to PheA as a control to evaluate the recognition of the amino group by PheA. The observed fluorescence at 327 nm was plotted vs the amino acid concentration and the curve analyzed with eq 1 using the KaleidaGraph computer program. In eq 1, ΔF<sub>obs</sub> is the observed change in fluorescence, ΔF<sub>max</sub>

$$\Delta F_{\text{obs}} = \Delta F_{\text{max}} / (1 + K_d / [S]) \quad (1)$$

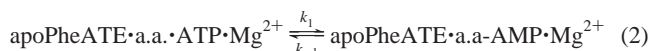
is the the total change in fluorescence, K<sub>d</sub> is the the apparent dissociation constant of the ligand, and [S] is the concentration of the amino acid ligand.

**ATP–PPi Exchange Assay.** Reactions for the ATP–PPi exchange assay were carried out at 30 °C in 100 μL total volume that contained 50 mM Tris (pH 7.5), 10 mM MgCl<sub>2</sub>, 4 mM ATP, 1 mM tris(2-carboxyethyl)phosphine (TCEP), 0.5 μM apoPheATE, 1 mM [<sup>32</sup>P]Na<sub>4</sub>-PPi, and varying concentrations of amino acid substrates. The reactions were initiated by addition of [<sup>32</sup>P]-pyrophosphate, allowed to proceed for 3–10 min, and then quenched by addition of a quenching solution (500 μL of 1.6% (w/v) activated charcoal, 4.46% (w/v) tetrasodium pyrophosphate, 3.5% perchloric acid in water). The charcoal was pelleted by centrifugation, washed twice with the quench solution without added charcoal, and then resuspended in 0.5 mL of water and submitted for liquid scintillation counting. The amount of bound radioactivity was converted into reaction velocity using the specific radioactivity of the [<sup>32</sup>P]-pyrophosphate. The initial velocity data were analyzed by using the Fortran HYPERL programs of Cleland (1979).<sup>26</sup>

**Amino Acid-Dependent ATP Usage.** A coupled, continuous, spectrophotometric assay for inorganic pyrophosphate (PPi) was employed to detect the rate at which PPi is released into solution.<sup>27</sup> Reactions were carried out at 30 °C in 100 μL total volume in a microtiter plate and contained 75 mM Tris, pH 7.5, 10 mM MgCl<sub>2</sub>, 200 μM 2-amino-6-mercapto-7-methylpurine ribonucleoside (MesG), 0.15 unit of purine nucleoside phosphorylase (PNP), 0.15 unit of inorganic pyrophosphatase (PPi-ase), 2 mM ATP, 2 μM apoPheATE (PheA or holoPheATE), and varying concentrations of the screened amino acid (50–2000 μM). Reactions were initiated by addition of the amino acid substrate after a 10-min incubation to allow the PPi-ase/PNP/MesG couple to remove any contaminating PPi or Pi. A SPECTRA max plus<sup>384</sup> microplate spectrometer was used to monitor absorbance at 360 nm (Δε<sub>360</sub> = 17.6 mM<sup>-1</sup> cm<sup>-1</sup>), and the software SOFTmax PRO 3.1 was used for data analysis. The steady-state kinetic

catalytic constants V<sub>max</sub> and K<sub>m</sub> for various amino acids were determined by using initial velocity techniques in conjunction with this continuous spectrophotometric assay.<sup>28</sup> The initial velocity data were analyzed by using the Fortran HYPERL programs of Cleland (1979).<sup>26</sup>

**Measurement of Single-Turnover Time Course for L-Aminoacyl–AMP Formation Catalyzed by ApoPheATE.** Single-turnover time courses for D-[<sup>14</sup>C]Phe–AMP, L-[<sup>3</sup>H]Trp–AMP, L-[<sup>14</sup>C]Tyr–AMP, L-[<sup>14</sup>C]Leu–AMP, and L-[<sup>14</sup>C]Pro–AMP formation were measured in a manner similar to that described in ref 13. All reactions were carried out at 30 °C using a rapid-quench flow apparatus from KinTek instruments. For reactions employed to define the kinetic profiles, the final concentrations after mixing (total volume 30 μL) were 35 μM apoPheATE enzyme, 6 μM radiolabeled amino acid, 5 mM MgCl<sub>2</sub>, 4 mM ATP, and 0.5 mM TCEP. The reaction mixture was quenched with 100 μL of 10% TCA (w/v) after incubation for a specified period of time (0.01–900 s). For reactions used to check the correlation between enzyme concentration and reaction rate, 66 μM was the final apoPheATE enzyme concentration. The reactions were TCA-quenched after 50 ms for D-Phe, 360 ms for L-Leu, 360 ms for L-Trp, and 60 s for L-Tyr reactions. All quench solutions were collected in a 2-mL Eppendorf tube. Following vigorous vortexing, the precipitated protein was pelleted by centrifugation for 20 min at 11600g at 4 °C. One microliter of the reaction supernatant was loaded onto a cellulose TLC plate (DC-Plastikfolien, EM Science) and developed in butanol/water/acetic acid 4:1:1 (v/v) (developing buffer A). Phosphorimages of TLC plates were obtained after 12–96-h exposure to BAS-MS2040 or BAS-TR2040 image plates and read by a Bio-Imaging Analyzer BAS1000 (Fuji). The image was analyzed densitometrically using the Image Gauge 3.0 software. The microscopic kinetic rate constants were obtained by fitting the single-turnover progress curve data to the enzymatic mechanistic scheme (eq 2) using the program DYNFIT by Petr Kuzmic.<sup>29</sup>



**Assay for Covalent Incorporation of Amino Acids into the T Domain of the HoloPheATE.** Amino acid incorporation into holo-carrier protein was quantified with a trichloroacetic acid (TCA) precipitation radioassay under single-turnover conditions. Each reaction was initiated by mixing 15 μL of 70 μM holoPheATE and 15 μL of 12 μM radiolabeled amino acid (see General for the specific radioactivity of the screened amino acids). The final concentrations after mixing (total volume 30 μL) were 35 μM holoPheATE enzyme, 6 μM L-(or D)-radiolabeled amino acid, 5 mM MgCl<sub>2</sub>, 4 mM ATP, and 0.5 mM TCEP. After incubation for 40 min, the reaction mixture was quenched with 100 μL of 10% TCA (w/v). Following vigorous vortexing, the precipitated protein was pelleted by centrifugation for 20 min at 11600g at 4 °C. The supernatant was separated from the pellet and the pellet washed with 2 × 500 μL of 10% TCA. The supernatant (combined with the solution from two washes) and the pellet (dissolved by formic acid) were assayed by scintillation counting using an LS6500 multi-purpose scintillation counter (Beckman).

**Measurement of Single-Turnover Time Course for HoloPheATE-Catalyzed Reactions.** Single-turnover time courses for holoPheATE catalyzed adenylation, thiolation, and epimerization of L-[<sup>14</sup>C]Tyr, L-[<sup>14</sup>C]Leu, and L-[<sup>3</sup>H]Trp were measured in a manner similar to that described in ref 13. The final concentrations after mixing (total volume 30 μL) were 35 μM holoPheATE enzyme, 6 μM radiolabeled amino acid, 5 mM MgCl<sub>2</sub>, 4 mM ATP, and 0.5 mM TCEP. After incubation for a specified period of time (0.01–2400 s), the reaction mixture was quenched with 100 μL of 10% TCA (w/v) and collected in a 2-mL Eppendorf tube. Following the same procedures as described in ref 13, the supernatant and the pellet were separated and the distributions of amino acid and amino acyl–AMP in supernatant, L-a.a., and D-a.a.

(26) Cleland, W. W. *Methods Enzymol.* **1979**, *63*, 103–137.

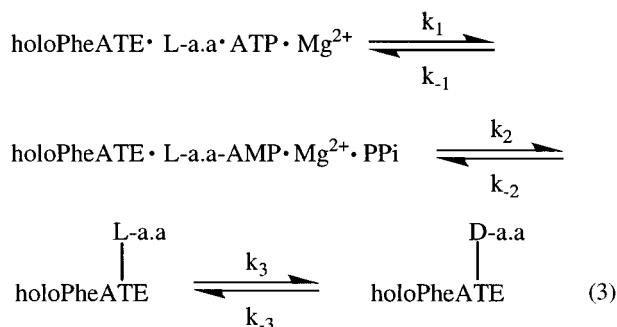
(27) (a) Keating, T. A.; Suo, Z.; Ehmann, D. E.; Walsh, C. T. *Biochemistry* **2000**, *39*, 2297–2306. (b) Ehmann, D. E.; Shaw-Reid, C. A.; Losey, H. C.; Walsh, C. T. *Proc. Natl. Acad. Sci. U.S.A.* **2000**, *97*, 2509–2514.

(28) We observed two sequential phases for the UV<sub>360 nm</sub> traces: a very rapid exponential phase that may be correlated to initial aminoacyl-adenylate formation and a slow and linear phase which is due to aminoacyl-adenylate release from the enzyme and further formation of aminoacyl-adenylate. The initial velocity we measured is the initial rate of the linear phase.

(29) Kuzmic, P. *Anal. Biochem.* **1996**, *237*, 260–273.

in pellet were analyzed by cellulose TLC plates and chiral TLC plates. The phosphorimages of TLC plates were analyzed densitometrically using the Image Gauge 3.0 software. L-Phe, L-Trp, L-Tyr, and L-Leu single-turnover reaction data were fitted to enzymatic mechanistic scheme (eq 3) using the program DYNAFIT.<sup>29</sup> D-Phe single-turnover reaction analysis was previously reported.<sup>13</sup>

**Calculation of  $\Delta G$  and  $\Delta G^\ddagger$ .** The transition-state free energy values



$\Delta G^\ddagger$  were calculated from the rate constants using eq 4, and the  $\Delta G$  values were calculated from the equilibrium constants using eq 5.<sup>30</sup> In eq 4,  $k_{\text{obs}}$  represents the observed kinetic rate constants,  $k_B$  represents the Boltzman constant,  $h$  represents the Plank constant, and  $T$  represents the temperature in kelvin. In eq 5,  $K_{\text{eq}}$  represents the derived equilibrium constants.

(30) Mehl, A.; Xu, Y.; Dunaway-Mariano, D. *Biochemistry* **1994**, *33*, 1093–1102.

$$\Delta G^\ddagger = -RT[\ln(k_{\text{obs}}) - \ln(k_B/Th)] \quad (4)$$

$$\Delta G = -RT \ln(K_{\text{eq}}) \quad (5)$$

**Assay of Epimerization Activity in apoPheATE by Using Aminoacyl-S-Pantetheines as Small-Molecule Surrogates.** All aminoacyl-S-pantetheines (a.a.-pant) were initially dissolved in 30  $\mu\text{M}$  trifluoroacetic acid (TFA), pH 3, and stored at  $-80^\circ\text{C}$  to minimize hydrolysis. Reactions (100  $\mu\text{L}$  each) contained 50 mM  $\text{K}^+\text{Hepes}$  (pH 7.5), 20  $\mu\text{M}$  apoPheATE, and 0.5–24 mM various a.a.-pants, which were incubated at  $30^\circ\text{C}$  and quenched at 30 min by adding 50  $\mu\text{L}$  of 10% TCA (w/v). The precipitated protein was pelleted by centrifugation at 11600g for 10 min. The supernatant was separated from the pellet and hydrolyzed by incubation with 100  $\mu\text{L}$  of 0.1 N potassium hydroxide for 30 min at  $70^\circ\text{C}$ . The supernatant was then injected onto a chiral HPLC column (ChiralPAK WH,  $4.6 \times 250$  mm, Chiral Technologies Inc) for analysis. A 2.5 mM  $\text{CuSO}_4$  buffer was employed to elute the column at a flow rate of 1 mL/min. The column eluant was monitored at UV 254 nm for aromatic amino acids and 230 nm for all other amino acids. The initial velocity data were analyzed by using the Fortran HYPERL programs.<sup>26</sup>

**Acknowledgment.** This work has been supported by the National Institutes of Health (Grant GM20011 to C.T.W.). M.D.B. was supported by a NIH postdoctoral fellowship. We thank Dr. Gerhard Wagner for the use of the PTI fluorescence system. We thank Dr. Suzanne Admiral and Rahul Kohli for a careful reading of the manuscript.

JA0166646